Available online at www.sciencedirect.com
SCIENCE DIRECT®
International Journal of Thermal Sciences 42 (2003) 973–982
International Journal of Thermal Sciences
www.elsevier.com/locate/ijts

The effect of surface mass transfer on mixed convection flow past a heated vertical flat permeable plate with thermophoresis

A. Selim [a], M.A. Hossain [a,*], D.A.S. Rees [b]

[a] *Department of Mathematics, University of Dhaka, Dhaka 1000, Bangladesh*
[b] *Department of Mechanical Engineering, University of Bath, Bath BA2 7AY, UK*

Received 2 June 2002; accepted 24 January 2003

Abstract

The present investigation deals with the effect of surface mass flux on mixed convective flow past a heated vertical flat permeable plate with thermophoresis. A nonuniform surface mass flux through the permeable surface has been considered. The governing equations, reduced to local nonsimilarity boundary layer equations using suitable transformations, have been integrated employing an implicit finite difference method together with the Keller-box technique (Keller [Annual Rev. Fluid Mech. 10 (1978) 417–433]). Perturbation techniques are employed to obtain the solutions near the leading edge as well as far from it. The perturbation solutions are compared with the finite difference solutions and found to be in excellent agreement. For fluids having the Prandtl number $Pr = 0.7$ and Schmidt number $Sc = 10.0$, numerical values of physical quantities, such as the local skin-friction coefficient, the local Nusselt number and the local Stanton number, are presented in tabular form for different values of the thermophoretic parameter τ against the local buoyancy parameter ξ for impermeable surfaces. Profiles of the dimensionless velocity, temperature and concentration distributions as well as the local skin-friction coefficient, local Nusselt number and the local Stanton number are shown graphically for various values of suction parameter, f_w, Schmidt number, *Sc* and the thermophoretic parameter τ.

Keywords: Mass transfer; Thermophoresis; Mixed convection; Permeable plate; Plate flow

1. Introduction

Thermophoresis is a phenomenon by which submicron sized particles suspended in a nonisothermal gas acquire a velocity relative to the gas in the direction of decreasing temperature. The velocity acquired by the particles is called the thermophoretic velocity and the force experienced by the suspended particles due to the temperature gradient is known as the thermophoretic force. The magnitudes of the thermophoretic force and velocity are proportional to the temperature gradient and depend on many factors like thermal conductivity of aerosol particles and the carrier gas. They also depend on the thermophoretic coefficient, the heat capacity of the gas and the Knudsen number. Thermophoresis causes small particles to deposit on cold surfaces. Repulsion of particles from hot objects also takes place and a particle-free layer is observed around hot bodies.

A common example of this phenomenon is blackening of the gas globe of a kerosene lantern. The temperature gradient developed between the flame and the gas globe drives the carbon particles produced in the combustion process towards the globe, where they deposit. There are several other practical situations where we come across this phenomenon, like gas "clean up", the corrosion of heat exchangers with attendant reduction of the heat transfer coefficient, the fouling of gas turbine equipment, the coagulation of condensing/evaporating aerosols. It also arises in determining particle trajectories in the exhaust gas from combustion devices and in the transpiration cooling of gas turbine blades, etc. Thermophoresis is considered to be the dominant mass transfer mechanism in the modified chemical vapour deposition process as currently used in the manufacturing of graded index optical fiber preforms. Thermophoretic deposition of radioactive particles is considered to be one of the important factors causing accidents in nuclear reactors.

The initial study of thermophoretic transport involved simple one-dimensional flows for the measurement of the

* Corresponding author.
E-mail address: anwar@udhaka.net (M.A. Hossain).

1290-0729/$ – see front matter
doi:10.1016/S1290-0729(03)00075-9

Nomenclature

C	species concentration in the boundary layer ..... $kg·m^{-2}$
C_{fx}	dimensionless local skin-friction coefficient
C_p	specific heat due to constant pressure ..... $J·kg^{-1}·K^{-1}$
$C_m, C_s, C_t, C_1, C_2, C_3$	constants in Eq. (7)
C_∞	species concentration of the ambient fluid
D	chemical molecular diffusivity
f	dimensionless stream function
f_w	dimensionless nonuniform surface mass flux
g	acceleration due to gravity ..... $m·s^{-2}$
Gr_x	local Grashof number for thermal diffusion
J_s	rate of transfer of species concentration ..... $kg·m^{-2}·s^{-1}$
k	thermophoretic coefficient defined by Eq. (7)
Kn	Knudsen number
Nu_x	local Nusselt number
Pr	Prandtl number
q_w	rate of heat transfer ..... W
Re_x	local Reynolds number
Sc	Schmidt number
St_x	local Stanton number
T	temperature of the fluid in the boundary layer K
T_∞	temperature of the ambient fluid ..... K
T_w	temperature at the surface ..... K
U_∞	free stream velocity ..... $m·s^{-1}$
u, v	the x- and y-components of the velocity field ..... $m·s^{-1}$
$V(x)$	transpiration velocity
V_T	thermophoretic velocity
x, y	axis in direction along and normal to the plate ..... m

Greek symbols

α	thermal diffusivity ..... $m^2·s^{-1}$
β	volumetric expansion coefficient of temperature
ρ	fluid density ..... $kg·m^{-3}$
ψ	stream function ..... $m^2·s^{-1}$
η	non-dimensional pseudo-similarity variable
ξ	the local buoyancy parameter
ν	kinematic coefficient of viscosity ..... $m^2·s^{-1}$
μ	fluid viscosity ..... Pa·s
τ_w	surface shear-stress ..... Pa
θ	dimensionless temperature function
ϕ	dimensionless species concentration function
λ_g, λ_p	thermal conductivity of gas and diffused particles, respectively
τ	thermophoretic parameter defined by Eq. (8)
κ	thermal conductivity ..... $W·m^{-1}·K^{-1}$

thermophoretic velocity and was undertaken by Goldsmith and May [2]. Talbot et al. [3] solved numerically for the velocity and temperature fields in the laminar boundary layer adjacent to a heated plate. Using several available theoretical expressions for the thermophoretic force, they calculated the trajectory of a particle entering the boundary layer. Measurements of the thickness of the particle-free layer next to the heated plate were compared with the calculated trajectories and it was found that the theory of Brock [4], modified slightly to fit the data for very small particles, gave the best overall agreement with the measurements. The first analysis of thermophoretic deposition in a geometry of engineering interest appears to be that of Hales et al. [5]. They solved the laminar boundary layer equations for simultaneous aerosol and steam transport to an isothermal vertical surface situated adjacent to a large body of an otherwise quiescent air-steam-aerosol mixture. Thermophoresis in laminar flow over a horizontal flat plate has been studied theoretically by Goren [6] where the analysis covered both cold and hot plate conditions. The laminar tube flow solution for thermophoretic deposition of small particles has been reported by Walker et al. [7]. The external transverse flow situation past a circular cylinder was analyzed by Homsy et al. [8] with the help of the Blasius series. Gokoglu and Rosner [9] arrived at a correlation for deposition rates in forced convection systems with variable properties, transpiration cooling and viscous dissipation. The thermophoretic deposition of the laminar slot jet on an inclined plate for hot, cold and adiabatic plate conditions with viscous dissipation effect were presented by Garg and Jayaraj [10]. Verms [11] has studied the deposition rates in cooled and uncooled turbines cascades. It was found that temperature difference between the wall and the gas could cause a 15-fold increase in deposition rate as compared with the case of adiabatic cascade. Shen [12] analyzed the problem of thermophoretic deposition of small particles on to cold surfaces in two-dimensional and axisymmetric cases and this is illustrated with examples of thermophoretic deposition of particles in flow past a cold cylinder and a sphere. Gokoglu and Rosner [13] studied the effect of particulate thermophoresis in reducing the fouling rate advantage of effusion cooling in gas turbines. Correlation has been developed to predict thermophoretically enhanced diffusional deposition rates, including the effects of transpiration cooling. Garg and Jayaraj [14] studied the thermophoretic transport of aerosol particles through a forced convection laminar boundary layer in cross flow over a cylinder for hot, cold and adiabatic wall conditions.

In the present paper we consider the effect of surface mass transfer on mixed convection flow past a heated vertical flat permeable surface in the presence of thermophoresis. Previous work on this topic includes papers by Epstein et al. [15], who carried out a thermophoretic analysis

of small particles in a free convection boundary layer adjacent to a cold vertical surface, and Mills et al. [16] and Tsai [17], who reported correlations for the deposition rate in the presence of thermophoresis and wall suction in laminar flow over a flat plate. Jia et al. [18] also investigated numerically the interaction between radiation and thermophoresis in forced convection laminar boundary-layer flow and natural convective laminar flow over a cold vertical flat plate in the presence of thermophoresis was solved numerically by Jayaraj [19] and Jayaraj et al. [20] for constant and variable properties, respectively. Finally, Chiou [21] analyzed the effect of thermophoresis on submicron particle deposition from a forced laminar boundary layer flow on to an isothermal moving plate through similarity solutions and this analysis was extended by Chiou and Cleaver [22] convection from a vertical isothermal cylinder.

In this investigation the combination of thermophoresis and a nonuniform surface mass flux through the permeable surface has been considered. Solutions of the momentum and energy equations yield the velocity and temperature distributions in the boundary layer, and these are used in the coupled concentration equation to calculate the rates of particle deposition. The governing partial differential equations are reduced to locally nonsimilar partial differential form by adopting transformations which are applicable to the forced convection, free convection and the intermediate mixed convection regimes. Solutions of the equations for both the forced and free convective cases are obtained by applying the perturbation method, while those for the mixed convection regime are obtained using the Keller-box technique (Keller, [1]). Our results are presented in terms of the skin-friction coefficient, C_{fx}; the rate of heat transfer, Nu_x; and the rate of species concentration, St_x in tabular form showing the effect of varying the governing dimensionless parameters, including the local buoyancy parameter, $\xi = Gr_x/Re_x^2$. Solutions obtained for the forced and free convective regimes are found to be in excellent agreement with the appropriate limits of the mixed convection regime solutions. Graphical presentations of the velocity, temperature and concentration profiles in addition to the skin-friction coefficient, the rate of heat transfer and the rate of species concentration are also given in order to show the effects of varying the permeability or suction/injection parameter, f_w, Schimdt number, Sc and the thermophoretic parameter, τ. Throughout the study Prandtl number is kept constant at 0.7 which represents air at 293 K and 1 atmosphere of pressure.

2. Formulation of the problem

Let us consider the two-dimensional steady laminar mixed convective flow of a viscous incompressible fluid along a heated vertical flat permeable plate in the presence of thermophoresis. The permeability is taken to be a variable depending on the distance measured from the leading edge. The external flow takes place in the direction parallel to the plate and has the uniform velocity U_∞. The temperature of the surface is held uniform at T_w which is higher than the ambient temperature T_∞.

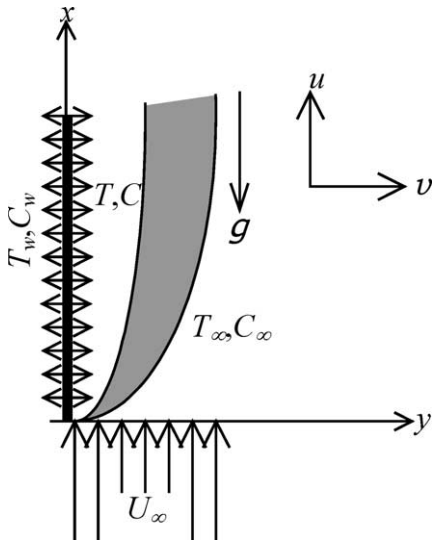

Fig. 1. The flow configuration and the coordinate system.

The species concentration at the surface is maintained uniform at C_w, which is taken to be zero and that of the ambient fluid is assumed to be C_∞. The effects of thermophoresis are being taken into account to help in the understanding of the mass deposition variation on the surface. The flow configuration and the coordinate system are as shown in Fig. 1.

We further assume:

(i) that the mass flux of particles is sufficiently small so that the main stream velocity and temperature fields are not affected by the thermophysical processes experienced by the relatively small number of particles,
(ii) that, due to the boundary layer behaviour, the temperature gradient in the y-direction is much larger than that in the x-direction and hence only that thermophoretic velocity component which is normal to the surface is of importance,
(iii) that the fluid has constant kinematic viscosity and thermal diffusivity, and that the Boussinesq approximation may be adopted for steady laminar flow, and
(iv) the particle diffusivity is assumed to be constant, and the concentration of particles is sufficiently dilute to assume that particle coagulation in the boundary layer is negligible.

Under the above assumptions, the equations for mass, momentum, energy and species conservation take the following form:

$$\frac{\partial u}{\partial x} + \frac{\partial v}{\partial y} = 0 \tag{1}$$

$$u\frac{\partial u}{\partial x} + v\frac{\partial u}{\partial y} = \nu\frac{\partial^2 u}{\partial y^2} + g\beta_T(T - T_\infty) \tag{2}$$

$$u\frac{\partial T}{\partial x}+v\frac{\partial T}{\partial y}=\frac{\nu}{Pr}\frac{\partial^2 T}{\partial y^2} \tag{3}$$

$$u\frac{\partial C}{\partial x}+v\frac{\partial C}{\partial y}=\frac{\nu}{Sc}\frac{\partial^2 C}{\partial y^2}-\frac{\partial}{\partial y}(V_T C) \tag{4}$$

The boundary conditions for the present problem are as follows:

$$u=0,\quad v=\pm V(x),\quad T=T_w,\quad C=C_w=0\quad \text{at } y=0$$
$$u\to U_\infty,\quad T\to T_\infty,\quad C\to C_\infty\quad \text{as } y\to\infty \tag{5}$$

where u and v are the fluid velocity components along the x- and y-axes (which are parallel and normal to the plate respectively), g is the gravitational force due to acceleration, β is the volumetric coefficient of thermal expansion, T is the temperature of the fluid in the boundary layer. C_p is the specific heat due to constant pressure. C is the species concentration in the boundary layer. ν, α and D being the kinematics coefficients of viscosity, thermal diffusivity and molecular diffusivity of the species concentration respectively. $Pr\ (=\nu/\alpha)$ is the Prandtl number and $Sc\ (=\nu/D)$ is the Schmidt number. In Eq. (5), $V(x)$ represents the permeability of the porous surface where its sign indicates suction (<0) or injection (>0). Here we confine our attention to the suction of fluid through the porous surface and for these we also consider that the transpiration function variable $V(x)$ is of the order of $x^{-1/2}$. In the present study we have neglected stratification, viscous dissipation and other additional effects.

The effect of thermophoresis is usually prescribed by means of an average velocity which a particle will acquire when exposed to a temperature gradient. In boundary layer flow, the temperature gradient in the y-direction is very much larger than in the x-direction, and therefore only the thermophoretic velocity in y-direction is considered. As a consequence, the thermophoretic velocity V_T, which appears in Eq. (4), may be expressed in the following form:

$$V_T=-\frac{k\nu}{T}\frac{\partial T}{\partial y} \tag{6}$$

where T is some reference temperature, the value of $k\nu$ represents the thermophoretic diffusivity, and k is the thermophoretic coefficient, which ranges in value from 0.2 to 1.2 as observed by Batchelor and Shen [23] and is defined from the theory of Talbot et al. [3] by:

$$k=\frac{2C_s(\lambda_g/\lambda_p+C_t Kn)[1+Kn(C_1+C_2e^{-C_3/Kn})]}{(1+3C_m Kn)(1+2\lambda_g/\lambda_p+2C_t Kn)} \tag{7}$$

where C_1, C_2, C_3, C_m, C_s, C_t are constants, λ_g and λ_p are respectively the thermal conductivities of gas and diffused particles, and Kn is the Knudsen number. As previously introduced by Mills et al. [16] and Tsai [17], the thermophoretic parameter, τ, is given by:

$$\tau=-\frac{k(T_w-T_\infty)}{T} \tag{8}$$

Typical values of τ are 0.01, 0.1 and 1.0 corresponding to approximate values of $-k(T_w-T_\infty)$ equal to 3, 30 and 300 K for a reference temperature of $T=300$ K.

In order to obtain a system of equations applicable to the entire regime of mixed convection, we now introduce the following continuous transformations to initiate the integration from forced to free convection regime as:

$$\psi=\nu Re_x^{1/2}(1+\xi)^{1/4}f(\xi,\eta)$$
$$T-T_\infty=(T_w-T_\infty)\theta(\xi,\eta),\qquad C=C_\infty\phi(\xi,\eta) \tag{9}$$
$$\xi=Gr_{x,T}/Re_x^2,\qquad \eta=\frac{y}{x}Re_x^{1/2}(1+\xi)^{1/4}$$

where ψ is the stream function that satisfies the continuity equation (1) and defined in the usual manner such that $u=\partial\psi/\partial y$ and $v=-\partial\psi/\partial x$. $f(\xi,\eta)$ is the dimensionless stream function, $\theta(\xi,\eta)$ is the dimensionless temperature of the fluid in the boundary layer region, $\phi(\xi,\eta)$ is the dimensionless species concentration of the fluid in the boundary layer region, η is the pseudo-similarity variable. The local buoyancy parameter ξ is small near the leading edge where the forced convection dominates and large in the downstream where free convection dominates; $Gr_x\ (=g\beta_T(T_w-T_\infty)x^3/\nu^2)$, and $Re_x\ (=U_\infty x/\nu)$ are, respectively, the local Grashof number for thermal diffusion and the local Reynolds number.

The transformations given in Eq. (9) are motivated by the forms of the forced and free convection similarity solutions of the equivalent convection problem. After substituting these transformations into Eqs. (2)–(4) one obtains the following non-similarity equatiuons:

$$f'''+p_1ff''-p_2f'^2+p_3\theta=\xi\left(f'\frac{\partial f'}{\partial\xi}-f''\frac{\partial f}{\partial\xi}\right) \tag{10.1}$$

$$\frac{1}{Pr}\theta''+p_1f-\theta'=\xi\left(f'\frac{\partial\theta}{\partial\xi}-\theta'\frac{\partial f}{\partial\xi}\right) \tag{10.2}$$

$$\frac{1}{Sc}\phi''+p_1f\phi'-\tau(\theta'\phi'+\theta''\phi)=\xi\left(f'\frac{\partial\phi}{\partial\xi}-\phi'\frac{\partial f}{\partial\xi}\right) \tag{10.3}$$

The corresponding boundary conditions transform into:

$$f(\xi,0)=2f_w\frac{(1+\xi)^{3/4}}{(2+3\xi)},\qquad f'(\xi,0)=0$$
$$f'(\xi,\infty)=(1+\xi)^{-1/2},\qquad \theta(\xi,0)=1 \tag{11}$$
$$\theta(\xi,\infty)=0,\qquad \phi(\xi,0)=0,\qquad \phi(\xi,\infty)=1$$

where

$$p_1=\frac{(2+3\xi)}{4(1+\xi)},\qquad p_2=\frac{\xi}{2(1+\xi)},\qquad p_3=\frac{\xi}{(1+\xi)} \tag{12}$$

In the above Eqs. (10.1)–(10.3) and in the boundary conditions (11), primes denote differentiation of the functions with respect to η and $f_w\ (=(2xV(x)/\nu)Re_x^{-1/2})$ is the dimensionless nonuniform surface mass flux, which is termed as the suction or injection parameter according to whether it is greater than or less than zero.

The quantities of physical interests are the surface shear-stress (τ_w), the rate of heat transfer (q_w) and the rate of transfer of species concentration (J_s) at the surface which may be obtained in terms of the local skin-friction coefficient, C_{fx}; the local Nusselt number, Nu_x; and the local Stanton number, St_x, respectively. They may be obtained from the following relations:

$$C_{fx}Re_x^{1/2} = \frac{\tau_w}{\rho U_\infty^2} = (1+\xi)^{3/4} f''(\xi, 0) \tag{13.1}$$

$$Nu_x Re_x^{-1/2} = \frac{q_w x}{(T_w - T_\infty)\kappa} = -(1+\xi)^{1/4}\theta'(\xi, 0) \tag{13.2}$$

$$St_x Re_x^{1/2} = -\frac{J_s}{U_\infty C_\infty} = \frac{1}{Sc}(1+\xi)^{1/4}\phi'(\xi, 0) \tag{13.3}$$

where

$$\tau_w = \mu\left(\frac{\partial u}{\partial y}\right)_{y=0}, \qquad q_w = -\kappa\left(\frac{\partial T}{\partial y}\right)_{y=0}$$

$$J_s = -D\left(\frac{\partial C}{\partial y}\right)_{y=0} \tag{14}$$

The system of Eqs. (10.1)–(10.3) and (11) have been solved by using the Keller-box. According to this method, the system of partial differential equations (10.1)–(10.3) are first converted to a system of seven first order partial differential equations by introducing new functions of η derivatives. This system is then expressed into finite-difference form and the resulting nonlinear system of algebraic equations is then linearized by the use of Newton's quasi linearization technique. The resulting linear difference equations along with the boundary conditions are finally solved by an efficient block-tridiagonal factorization method introduced by Keller [1]. For a given ξ, the iterative procedure was stopped to give the final velocity, temperature and concentration distribution when the difference in computing these functions in the next procedure becomes less than 10^{-5}, i.e., $|\delta f^i| \leqslant 10^{-6}$, where the superscript i denotes the iteration number. For these computations, a non-uniform grid in the η direction has been used by considering $\eta_j = \sinh\{(j-1)/a\}$, where $j = 1, 2, 3, \ldots, J$. Here $J = 251$ and $a = 100$ had been chosen in order to obtain quick convergence and thus save computational time and memory space. In the present investigation scheme, values of ξ are increased with the increment $\Delta\xi = 0.01$ until the asymptotic values for the skin-friction, heat transfer rate and species concentration rate were reached for every variation of the pertinent parameter τ, f_w and Sc for $Pr = 0.7$.

Results obtained by this method are presented in Tables 2 and 3 and compared with the solutions obtained by other methods. Also the effect of varying the different governing parameters is discussed later.

Table 1 present a comparison of the local Stanton number ($St_x Re_x^{1/2}\sqrt{2}$) obtained in the present investigation and those obtained earlier by Mills et al. [16] and Tsai [17]. It is clearly observed that good agreement between the results exists. This lends confidence in the present numerical method.

Table 1
Comparison of $St_x Re_x^{1/2}\sqrt{2}$ with those of Mills et al. [16] and Tsai [17] for different $\tau = 0.01$, 0.1, 10.0 and $f_w = 0.0$, 0.5, 1.0 at $\xi = 0.0$, $Sc = 1{,}000$ and $Pr = 0.7$

τ	f_w	Mills et al. [16]	Tsai [17]	Present work
0.01	1.0	0.7091	0.7100	0.6964
0.01	0.5	0.3559	0.3565	0.3500
0.01	0.0	0.0029	0.0029	0.0030
0.1	1.0	0.7265	0.7346	0.7307
0.1	0.5	0.3767	0.3810	0.3738
0.1	0.0	0.0277	0.0275	0.0279
1.0	1.0	0.8619	0.9134	0.9340
1.0	0.5	0.5346	0.5598	0.5979
1.0	0.0	0.2095	0.2063	0.2096

Table 2
Numerical values of the local skin-friction coefficient, $C_{fx}Re_x^{1/2}$; and the local Nusselt number, $Nu_x Re_x^{-1/2}$ obtained by different methods for $\tau = 0.0$, $Pr = 0.7$, $Sc = 10.0$, $f_w = 0.0$ against different values of ξ

ξ	$C_{fx}Re_x^{1/2}$		$Nu_x Re_x^{-1/2}$	
	Finite diff.	Small & large ξ	Finite diff.	Small & large ξ
0.0	0.33333	0.33266[s]	0.29538	0.29429[s]
0.1	0.44909	0.44606[s]	0.31646	0.31526[s]
0.15	0.50299	0.49703[s]	0.32552	0.32321[s]
0.2	0.55084	0.54298[s]	0.33298	0.32866[s]
0.25	0.60016	0.58146[s]	0.34040	0.33011[s]
0.5	0.81885		0.36944	
1.0	1.20174		0.41090	
2.0	1.85598	1.83413[a]	0.46620	0.46318[a]
3.0	2.43236	2.41953[a]	0.50559	0.50427[a]
4.0	2.96220	2.95300[a]	0.53693	0.53654[a]
5.0	3.45957	3.45615[a]	0.56327	0.56347[a]

[s] For small ξ.
[a] For large ξ.

3. Results and discussion

For this present problem numerical computations have been carried out by employing the finite difference method known as the Keller-box method for all ξ, and the perturbation series solution method for small and large ξ.

A comparison of the local Stanton number ($St_x Re_x^{1/2}\sqrt{2}$) obtained in the present work and those obtained earlier by Mills et al. [16] and Tsai [17] has been shown earlier in Table 1. Comparison also taken for the values of the local skin-friction coefficient and the local Nusselt number obtained in the present work with that of Merkin [24] for the case of small and large ξ with $Pr = 1$. It is clearly seen that there is excellent agreement between the respective results.

In the forced convection regime, relatively near the leading edge, i.e., for small ξ, the functions given in Eqs. (12) take the following form:

$$p_1 = \frac{1}{2}, \qquad p_2 = 0, \qquad p_3 = \xi \tag{15}$$

As ξ is small, the solutions of the governing equations of this regime may be obtained by using the perturbation method treating ξ as the perturbation parameter. Hence we

Table 3
Numerical values of the local Stanton number, $St_x Re_x^{1/2}$ obtained by different methods against different values of ξ for $\tau = 0.1$, 0.5, 1.0 and $Pr = 0.7$, $Sc = 10.0$, $f_w = 0.0$

ξ	$St_x Re_x^{1/2}$					
	Finite diff.	Small & large ξ	Finite diff.	Small & large ξ	Finite diff.	Small & large ξ
	$\tau = 0.1$		$\tau = 0.5$		$\tau = 1.0$	
0.0	0.08690	0.08680[s]	0.14955	0.14836[s]	0.22660	0.22598[s]
0.1	0.09545	0.09525[s]	0.16166	0.16062[s]	0.24267	0.24224[s]
0.15	0.09905	0.09840[s]	0.16690	0.16515[s]	0.24971	0.24824[s]
0.2	0.10200	0.10050[s]	0.17112	0.16804[s]	0.25533	0.25206[s]
0.25	0.10494	0.10091[s]	0.17536	0.16515[s]	0.26182	0.25233[s]
0.5	0.11631		0.19167		0.28289	
1.0	0.13227		0.21833		0.31387	
2.0	0.15312	0.15267[a]	0.24479	0.24351[a]	0.35496	0.35150[a]
3.0	0.16773	0.16763[a]	0.26812	0.26595[a]	0.38417	0.38186[a]
4.0	0.17923	0.17928[a]	0.28293	0.28351[a]	0.40742	0.40576[a]
5.0	0.18883	0.18896[a]	0.29704	0.29814[a]	0.42697	0.42573[a]

[s] For small ξ.
[a] For large ξ.

expand the functions $f(\xi,\eta)$, $\theta(\xi,\eta)$ and $\phi(\xi,\eta)$ in powers of ξ and solutions of those equations are obtained by using the Natscheim–Swigert iteration technique together with the sixth order implicit Runge–Kutta–Butcher initial value solver. Here we integrated the equations up to order $O(\xi^4)$.

Once the values of the functions $f_i(\eta)$, $\theta_i(\eta)$ and $\phi_i(\eta)$ for $i = 0, 1, 2, \ldots$ and their derivatives at $\eta = 0$ are known, the quantities C_{fx}, Nu_x and St_x can now be calculated respectively from the following expressions:

$$C_{fx}Re_x^{1/2} = f''(\xi,0) = f_0'' + \xi f_0''^2 + \xi^2 f_0''^3 + \cdots \quad (16.1)$$

$$Nu_x Re_x^{-1/2} = -\theta'(\xi,0) = -\left[\theta_0' + \xi\theta_0'^2 + \xi^2\theta_0'^3 + \cdots\right] \quad (16.2)$$

and

$$St_x Re_x^{1/2} = \frac{1}{Sc}\phi'(\xi,0) = \frac{1}{Sc}\left[\phi_0' + \xi\phi_0'^2 + \xi^2\phi_0'^3 + \cdots\right] \quad (16.3)$$

The resulting values of the local skin-friction coefficient, the local Nusselt number and the local Stanton number are entered in Tables 2 and 3, and compared with the corresponding values obtained from the finite difference solution.

For example, for $Pr = 1.0$, $f_w = 0.0$, and $\tau = 0.0$, the numerical values of the local skin-friction coefficient and the local Nusselt number for different values of ξ can be obtained from the following expression:

$$C_{fx}Re_x^{1/2} = \left[(0.3325) + \xi(1.1454) + \xi^2(-0.8947) + \cdots\right] \quad (17.1)$$

$$Nu_x Re_x^{-1/2} = -\left[(-0.3325) + \xi(-0.2706) + \xi^2(0.4608) + \cdots\right] \quad (17.2)$$

According to Merkin [24] the skin-friction coefficient and the heat transfer coefficient for $Pr = 1.0$ are:

$$C_{fx} = \left[(0.3321) + \xi(1.1466) + \xi^2(-0.8979) + \cdots\right] \quad (18.1)$$

$$Nu_x = \left[(0.3321) + \xi(0.2711) + \xi^2(-0.4627) + \cdots\right] \quad (18.2)$$

It can be seen that the relations (17.1), (17.2) and (18.1), (18.2) are in excellent agreement.

In the free convection regime, i.e., at large ξ, the functions given in Eqs. (12) take the following form:

$$p_1 = \frac{3}{4}, \qquad p_2 = \frac{1}{2}, \qquad p_3 = 1 \quad (19)$$

In this case, we expand the functions $f(\xi,\eta)$, $\theta(\xi,\eta)$ and $\phi(\xi,\eta)$ in powers of $\xi^{-i/4}$ and the solution methodology applied in solving above sets of equations is same as for the small ξ equations. Here we integrated the equations up to order $O(\xi^{-2/4})$.

As before, when we know the values of the functions $f_i(\eta)$, $\theta_i(\eta)$ and $\phi_i(\eta)$ for $i = 0, 1, 2, \ldots$ and their derivatives at $\eta = 0$, we may calculate the local skin-friction coefficient, C_{fx}; the local Nusselt number, Nu_x; and the local Stanton number St_x in the downstream regime from the following relations:

$$C_{fx}Re_x^{1/2} = \xi^{3/4} f''(\xi,0) = \xi^{3/4}\left[f_0'' + \xi^{-1/4} f_0''^2 + \xi^{-2/4} f_0''^3 + \cdots\right] \quad (20.1)$$

$$Nu_x Re_x^{-1/2} = -\xi^{1/4}\theta'(\xi,0) = -\xi^{1/4}\left[\theta_0' + \xi^{-1/4}\theta_0'^2 + \xi^{-2/4}\theta_0'^3 + \cdots\right] \quad (20.2)$$

$$St_x Re_x^{1/2} = \frac{1}{Sc}\xi^{1/4}\phi'(\xi,0) = \frac{1}{Sc}\left[\phi_0' + \xi^{-1/4}\phi_0'^2 + \xi^{-2/4}\phi_0'^3 + \cdots\right] \quad (20.3)$$

These asymptotic solutions are compared with the solution of the finite difference method in Tables 2, 3.

For $Pr = 1.0$, $f_w = 0.0$, and $\tau = 0.0$, the asymptotic values of the local skin-friction coefficient and the local Nusselt number for different values of ξ can now be obtained from the following expression:

$$C_{fx}Re_x^{1/2} = \left[(0.9010) + \xi^{-2/4}(0.1345) + \cdots\right] \quad (21.1)$$

$$Nu_x Re_x^{-1/2} = -\left[(-0.4024) + \xi^{-2/4}(-0.0499) + \cdots\right] \quad (21.2)$$

According to Merkin [24] the asymptotic values of the local skin-friction coefficient and the heat transfer coefficient for $Pr = 1.0$ are:

$$C_{fx} = \left[(0.9082) + \xi^{-2/4}(0.1173) + \cdots\right] \quad (22.1)$$

$$Nu_x = \left[(0.4010) + \xi^{-2/4}(0.0503) + \cdots\right] \quad (22.2)$$

The above set of expressions (21.1), (21.2) and (22.1), (22.2) are also in good agreement.

In Table 2 we have entered the numerical values of the local skin-friction coefficient and the local Nusselt number that are found by the above mentioned three methods which corresponds to an impermeable surface condition ($f_w = 0.0$) for fluids having Prandtl number $Pr = 0.7$, Schmidt number $Sc = 10.0$ and the thermophoretic parameter $\tau = 0.0$ against different values of $\xi \in [0, 5]$. Since τ is significant for the local Stanton number, so in Table 3 we have depicted the numerical value of the local Stanton number and compared by other methods for three values of thermophoretic parameter $\tau = 0.1$, 0.5, 1.0 with the same parameter cases as considered in Table 2. We observe that when ξ increases, the local skin-friction coefficient, the local Nusselt number and the local Stanton numbers also increase in a manner consistent with a free convection boundary layer. Also, from Tables 2 and 3, it may be seen clearly that both the small and large ξ solutions compare very well with the Keller box computations at intermediate values of ξ, thereby lending confidence to the accuracy of our results.

Values of dimensionless velocity, temperature and concentration distributions are shown in Figs. 2(a)–(c), respectively, for values of the local buoyancy parameter $\xi = 0.0$, 0.5, 1.0, 2.0 and 5.0 while $Pr = 0.7$, $Sc = 1000.0$, $f_w = 0.0$, and $\tau = 0.1$. From Fig. 2(a), it can be observed that, when $\xi = 0$, the velocity profile corresponds to pure forced convection, but when $\xi > 1$, free convective effects have become sufficiently strong to produce a well-defined maxiumum velocity, which is higher than that of the free stream. At large values of ξ forced convection effects are negligible. From Fig. 2(b) we see that the boundary layer becomes thinner as ξ increases. This is due to the fact that the streamwise velocity increases as ξ increases, which means that heat is less able to conduct away from the surface. For hot surfaces, thermophoresis tends to blow the concentration boundary layer away from the surface since a hot surface repels the sub-micron sized particles from it, thereby forming a relatively particle-free layer near the surface. As a consequence, the species concentration distribution is formed just outside the particle-free layer. This is of particular benefit in processes that require extreme cleanliness of the surface. Fig. 2(c) shows that the particle-free layer thickness decreases as the buoyancy parameter ξ increases.

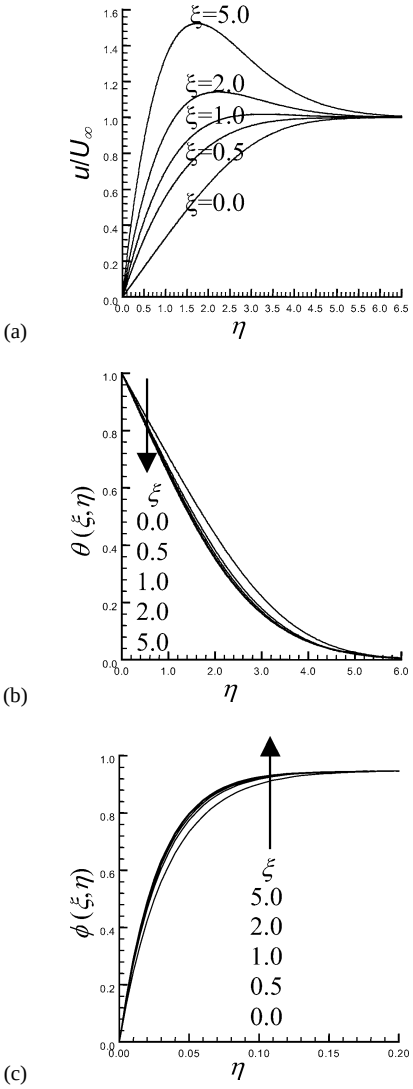

Fig. 2. (a)–(c): Dimensionless velocity, temperature and concentration profiles, respectively, for $\xi = 0.0$, 0.5, 1.0, 2.0 and 5.0, for $Pr = 0.7$, $Sc = 1000.0$, $f_w = 0.0$, and $\tau = 0.1$.

Figs. 3(a)–(c) illustrate the effect of varying the strength of the suction of fluid through the permeable surface ($f_w > 0$) on the velocity, temperature and concentration profiles, respectively. The imposition of wall fluid suction ($f_w > 0$) for this problem has the effect of reducing both the thicknesses of the temperature and concentration boundary layer thicknesses, and reducing the streamwise velocity at each finite value of η. The decreasing thickness of the concentration layer is caused by two effects: (i) the direct action of suction, and (ii) the indirect action of suction causing a thinner thermal boundary layer, which corresponds to a higher temperature gradients, a consequent increase in the thermophoretic force and higher concentration gradients. Figs. 4(a)–(c) show the corresponding effect of varying f_w on the skin-friction coefficient $C_{fx}Re_x^{1/2}(f''(0))$, the wall heat transfer $Nu_x Re_x^{-1/2}(-\theta'(0))$ and the wall deposition flux $St_x Re_x^{1/2}(\phi'(0))$, respectively. These figures also con-

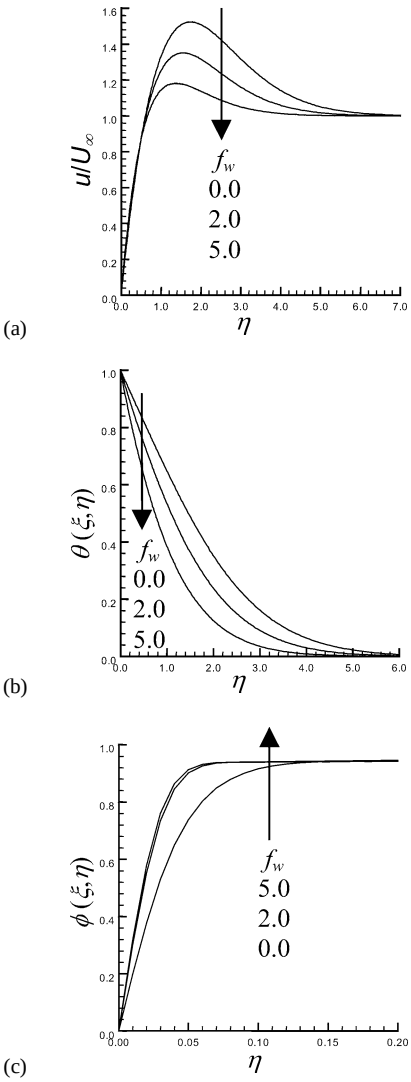

Fig. 3. (a)–(c): Effect of different values of f_w on velocity, temperature and concentration profiles, respectively, for $f_w = 0.0$, 2.0 and 5.0 while $\xi = 5.0$, $Sc = 1000.0$, $Pr = 0.7$, and $\tau = 0.1$.

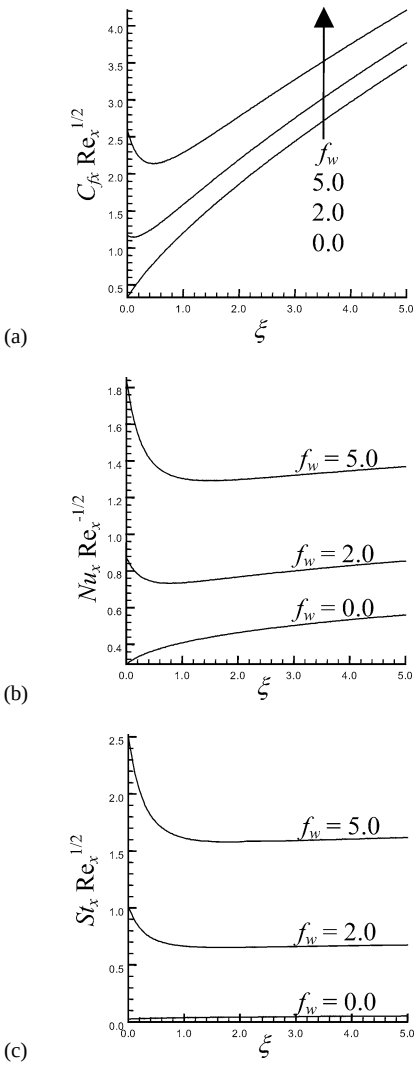

Fig. 4. (a)–(c): Effect of different values of f_w on the skin-friction, wall heat transfer and wall deposition flux, respectively, as a function of ξ for $f_w = 0.0$, 2.0 and 5.0 while $Sc = 1000.0$, $Pr = 0.7$, and $\tau = 0.1$.

firm that as f_w increases, the skin-friction coefficient, the wall heat transfer and the wall deposition flux all increase.

In Figs. 5(a) and 6(a) we have shown typical concentration profiles for various values of the Schmidt number *Sc* and the thermophoretic parameter τ, respectively, in the absence of surface suction. It is clear from Fig. 5(a) that the concentration layer thickness decreases as the Schmidt number *Sc* increases; this is analogous to the effect of increasing the Prandtl number on the thickness of a thermal boundary layer. For the parametric conditions used in Fig. 6(a), the effect of increasing the thermophoretic parameter τ is limited to increasing slightly the wall slope of the concentration profile for $\eta < 1.0$ but decreasing the concentration for values of $\eta > 1.0$. Of more importance is the surface mass flux, and the separate effect of varying *Sc* and τ on the wall deposition flux coefficient are shown in Figs. 5(b) and 6(b), respectively. In Fig. 5(b) we see that increasing values of *Sc* decrease the surface mass flux for all values of ξ; this effect is particularly strong. Conversely, the increase of the surface mass flux with variations in τ are relatively small.

4. Conclusions

The effect of surface mass transfer on mixed convection flow past a heated vertical flat permeable plate with thermophoresis has been investigated theoretically. The nonsimilar equations which govern the flow in the intermediate mixed convection regime, the forced convection regime and the free convection regime are obtained by using appropriate transformations. Solutions for the forced convection regime and the free convection regime have been obtained using perturbation methods and have been compared favourably with the solution for the mixed convection regime obtained by the Keller-box method. The numerical results have been provided in terms of the local skin-friction coefficient, local

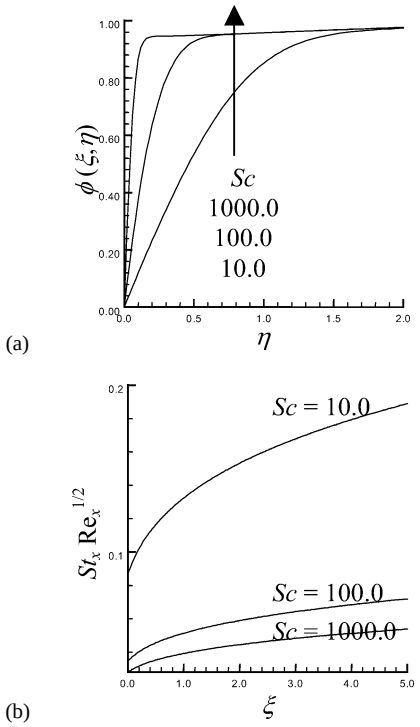

Fig. 5. (a) Effect of different values of *Sc* on the concentration profiles for $Sc = 10.0$, 100.0 and 1000.0, with $Pr = 0.7$, $\xi = 5.0$, $\tau = 0.1$ and $f_w = 0.0$. (b) Effect of different values of *Sc* on the wall deposition flux as a function of ξ for $Sc = 10.0$, 100.0 and 1000.0, with $Pr = 0.7$, $\tau = 0.1$ and $f_w = 0.0$.

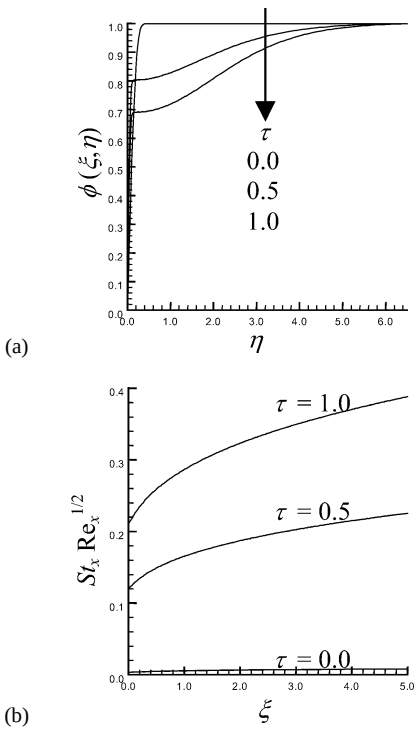

Fig. 6. (a) Effect of different values of τ on the concentration profiles for $\tau = 0.0$, 0.5 and 1.0, with $Sc = 1000.0$, $\xi = 5.0$, $Pr = 0.7$, and $f_w = 0.0$. (b) Effect of different values of τ on the wall deposition flux as functions of ξ for $\tau = 0.0$, 0.5 and 1.0, with $Sc = 1000.0$, $Pr = 0.7$, and $f_w = 0.0$.

Nusselt number and local Stanton number with impermeable surface condition for fluids having Prandtl number $Pr = 0.7$, Schmidt number $Sc = 10.0$ and for different values of thermophoretic parameter τ as functions of the local buoyancy parameter $\xi \in [0, 5]$. Excellent agreement has been observed between the results obtained by the two different methods.

From the present investigation the following conclusions may be drawn:

- In the mixed convection regime the values of the local skin-friction coefficient, the local Nusselt number and the local Stanton number increase when the value of the local buoyancy parameter ξ increases.
- As ξ increases both the temperature and concentration boundary layers decrease in thickness.
- Wall suction was found to decrease the strength of the streamwise flow and to decrease both the thermal and concentration boundary layer thicknesses.
- As the Schmidt number *Sc* increases, the concentration boundary layer becomes thinner and the surface mass flux increases.
- As the thermophoretic parameter, τ, increases, the surface mass flux increases.

Acknowledgement

One of the authors (A. Selim) would like to express her gratitude to the National Science and Technology Ministry, Dhaka for providing financial support during the period in which the research was undertaken.

References

[1] H.B. Keller, Numerical methods in boundary layer theory, Annual Rev. Fluid Mech. 10 (1978) 417–433.
[2] P. Goldsmith, F.G. May, Diffusiophoresis and thermophoresis in water vapour systems, in: C.N. Davies (Ed.), Aerosol Science, Academic Press, London, 1966, pp. 163–194.
[3] L. Talbot, R.K. Chenge, A.W. Schefer, D.R. Willis, Thermophoresis of particles in a heated boundary layer, J. Fluid Mech. 101 (1980) 737–758.
[4] J.R. Brock, On the theory of thermal forces acting on aerosol particles, J. Colloid Sci. 17 (1962) 768–770.
[5] J.M. Hales, L.C. Schwendiman, T.W. Horst, Aerosol transport in a naturally-convected boundary layer, Internat. J. Heat Mass Transfer 15 (1972) 1837–1849.
[6] S.L. Goren, Thermophoresis of aerosol particles in the laminar boundary layer on a flat plate, J. Colloid Interface Sci. 61 (1977) 77–85.
[7] K.L. Walker, G.M. Homsy, F.T. Geyling, Thermophoretic deposition of small particles in laminar tube flow, J. Colloid Interface Sci. 69 (1979) 138–147.
[8] G.M. Homsy, F.T. Geyling, K.L. Walker, Blasius series for thermophoretic deposition of small particles, J. Colloid Interface Sci. 83 (1981) 495–501.
[9] S.A. Gokoglu, D.E. Rosner, Correlation of thermophoretically-modified small particle diffusional deposition rates in forced convection systems with variable properties, transpiration cooling and/or

viscous dissipation, Internat. J. Heat Mass Transfer 27 (1984) 639–646.

[10] V.K. Garg, S. Jayaraj, Thermophoresis of aerosol particles in laminar flow over inclined plates, Internat. J. Heat Mass Transfer 31 (1988) 875–890.

[11] G. Verms, Thermophoresis-enhanced deposition rates in combustion turbine blade passages, J. Engrg. Power 101 (1979) 542–548.

[12] C. Shen, Thermophoretic deposition of particles on to cold surfaces in two-dimensional and axi-symmetric flows, J. Colloid Interface Sci. 127 (1989) 104–115.

[13] S.A. Gokoglu, D.E. Rosner, Correlation of thermophoretically-modified small particle diffusional deposition rates in forced convection systems with variable properties, transpiration cooling and/or viscous dissipation, Internat. J. Heat Mass Transfer 27 (1984) 639–646.

[14] V.K. Garg, S. Jayaraj, Thermophoretic deposition over a cylinder, Internat. J. Engrg. Fluid Mech. 3 (1990) 175–196.

[15] M. Epstein, G.M. Hauser, R.E. Henry, Thermophoretic deposition of particles in natural convection flow from a vertical plate, J. Heat Transfer 107 (1985) 272–276.

[16] A.F. Mills, X. Hang, F. Ayazi, The effect of wall suction and thermophoresis on aerosol-particle deposition from a laminar boundary-layer on a flat-plate, Internat. J. Heat Mass Transfer 27 (1984) 1110–1113.

[17] R. Tsai, A simple approach for evaluating the effect of wall suction and thermophoresis on aerosol particle deposition from a laminar flow over a flat plate, Internat. Commun. Heat Mass Transfer 26 (1999) 249–257.

[18] G. Jia, J.W. Cipolla, Y. Yener, Thermophoresis of a radiating aerosol in laminar boundary-layer flow, J. Thermophys. Heat Transfer 6 (1992) 476–482.

[19] S. Jayaraj, Finite difference modelling of natural convection flow with thermophoresis, Internat. J. Numer. Methods Heat Fluid Flow 9 (1999) 692–704.

[20] S. Jayaraj, K.K. Dinesh, K.L. Pillai, Thermophoresis in natural-convection with variable properties, Heat Mass Transfer 34 (1999) 469–475.

[21] M.C. Chiou, Effect of thermophoresis on sub-micron particle deposition from a forced laminar boundary layer flow on to an isothermal moving plate, Acta Mech. 129 (1998) 219–229.

[22] M.C. Chiou, J.W. Cleaver, Effect of thermophoresis on sub-micron particle deposition from a laminar forced convection boundary layer flow on to an isothermal cylinder, J. Aerosol. Sci. 27 (1996) 1155–1167.

[23] G.K. Batchelor, C. Shen, Thermophoretic deposition of particles in gas flowing over cold surfaces, J. Colloid Interface Sci. 107 (1985) 21–37.

[24] J.H. Merkin, The effect of buoyancy forces on the boundary-layer flow over a semi-infinite vertical flat plate in a uniform stream, J. Fluid Mech. 35 (3) (1969) 439–450.